frontiers | Frontiers in Earth Science

ORIGINAL RESEARCH
published: 07 June 2022
doi: 10.3389/feart.2022.938765

Development Characteristics of Silurian Strike-Slip Faults and Fractures and Their Effects on Drilling Leakage in Shunbei Area of Tarim Basin

*Haiying Li**

Exploration and Development Research Institute, Sinopec Northwest Oilfield Branch, Urumqi, China

In recent years, the Ordovician fault-controlled fracture-cavity reservoirs developed in the basement strike-slip fault zone in the Shunbei area of the Tarim Basin has achieved major breakthroughs. However, during the drilling process of the strike-slip fault zone in the Shunbei area, the problem of mud leakage in the frequently interbedded Silurian sandstone and mudstone strata overlying the Ordovician target layer is very significant, and it has seriously affected the normal drilling and wellbore stability. In this study, taking the Silurian of the No. A Strike-slip Fault Zone in the Shunbei area as an example, the development characteristics of strike-slip faults and fractures, the strength of the *in-situ* stress field, and the influence of these factors on the drilling mud leakage were systematically studied using 3D seismic, logging, drilling, logging, well log, and engineering construction data. The results show that the mud leakage in strata S_{1t} is significantly larger than that in S_{1k}, and the leakage amount in sandy mudstone is the largest; the strong strike-slip extension developed the negative flower-shaped normal faults and the right-order swan-type faults and caused serious stratigraphic fragmentation. The amount of mud leakage increases with the increase of fault distance. Moreover, the closer to the fault, the higher the frequency and amount of mud leakage. When the distance between the wellbore and the fault exceeds 300 m, the possibility of mud leakage decreases significantly. The Silurian S_{1t} is dominated by high-angle and vertical tension-shear fractures with good opening; while the S_{1k} is dominated by low-angle structural and horizontal bedding fractures. The differences in fracture type cause the mud leakage in S_{1t} to be significantly larger than that of S_{1k}. In addition, the fracture development intervals identified by the R/S-FD method are in good agreement with the mud leakage intervals, which further indicates that the degree of fracture development is the key factor leading to the drilling mud leakage. The study also found that the degree of fracture development and the difference in horizontal principal stresses are the dominant factors leading to high Silurian mud leakage.

Keywords: tarim basin, shunbei area, silurian, strike-slip fault, fracture characteristics, drilling leakage analysis

OPEN ACCESS

Edited by:
Shuai Yin,
Xi'an Shiyou University, China

Reviewed by:
Teng Zhao,
China University of Geosciences, China
Li Ang,
Jilin University, China

****Correspondence:***
Haiying Li
lihaiying202205@163.com

Specialty section:
This article was submitted to Structural Geology and Tectonics, a section of the journal Frontiers in Earth Science

Received: *08 May 2022*
Accepted: *13 May 2022*
Published: *07 June 2022*

Citation:
Li H (2022) Development Characteristics of Silurian Strike-Slip Faults and Fractures and Their Effects on Drilling Leakage in Shunbei Area of Tarim Basin. Front. Earth Sci. 10:938765. doi: 10.3389/feart.2022.938765

INTRODUCTION

Basement strike-slip fault zones in petroliferous basins are an important type of high-yield hydrocarbon enrichment zone (Jiao, 2017; Jiao, 2018; Santosh and Feng, 2020; Qi et al., 2021). Controlled by the action of basement strike-slip structures, the deformation of strike-slip structures is usually confined to a narrow strip along the main fault strike. Furthermore, most of them are linear, belt-shaped, geese-shaped, S-shaped or reverse-S-shaped on the plane, and have a flower-like structure on the cross-section. In three-dimensional space, the main faults often show the phenomenon of "ribbon effect" and "dolphin effect", and indirectly cause the strike-slip fault zone to have obvious segmentation differences. Then, "strike-slip extension", "strike-slip overhang" and "strike-slip translation" can be identified (Deng, et al., 2019a; Li et al., 2019; Fan et al., 2020; Ding et al., 2021; Li, 2022). Moreover, they are affected by multi-stage tectonic movements and multiple sets of detachment layers, so that the deformation styles of strike-slip faults in different tectonic layers have obvious stratification differences (Li et al., 2020; Xue et al., 2021).

Strike-slip fault zones often exhibit the characteristics of "planar segmentation, vertical stratification, multi-period superposition, and variable stress" (Deng et al., 2018; Deng et al., 2019b; He et al., 2020; Hower and Groppo., 2021; Zhan Zhao et al., 2021). They are also the internal mechanism of the "reservoir and hydrocarbon-controlling effect" of strike-slip faults. The multi-stage activities of strike-slip faults have an important impact on the formation of fracture systems and the improvement of petrophysical properties in carbonate rock, shale, and tight sandstone reservoirs (Han et al., 2016; Zhao et al., 2019; Mohammed et al., 2021). In addition, fault activity can also cause the wellbore instability of drilling near the strike-slip fault zone (such as mud loss, wellbore collapse, falling blocks and sticking, etc.) (Al-Ajmi and Zimmerman., 2006; Chen et al., 2014; Yin et al., 2015; Yan and Zhao, 2018; Yin et al., 2018; Zheng et al., 2020; Chen et al., 2021; Gao, 2021).

The Paleozoic and Mesozoic Cenozoic sedimentary strata in Shunbei area of Tarim Basin are well developed, and Permian volcanic rocks and upper Ordovician intrusive dolerite bodies are also developed. Among them, the carbonate rocks of the Middle and Lower Ordovician are the target layers for oil and gas exploration, while the overlying Silurian sand-mudstone interbedded strata, Permian volcanic rocks, and Upper Ordovician diabase strata have serious wellbore instability. Especially in the Silurian sand-mudstone interbedded strata, the leakage of drilling mud is the most serious, and the phenomenon of "nine leakages in ten wells" is remarkable. Therefore, with the continuous expansion of the oil and gas exploration scope of the strike-slip fault zone in the Shunbei area, studies have found that the Silurian sand-mudstone strata overlying the Ordovician target layer have low stress bearing capacity, developed faults, and developed a large number of complex open and closed fracture systems (Yin et al., 2020). Therefore, the random multi-point mud leakage in the whole well section is very serious, which has seriously affected the normal drilling and wellbore stability. *In-situ* stress is the key factor of leakage (Li et al., 2011).

In this study, taking the Silurian of the No. A Strike-slip Fault Zone in the Shunbei area as an example, the theory of reservoir geomechanics was used to analyze the development characteristics of strike-slip faults and fractures, as well as the distribution characteristics of *in-situ* stress fields, and their relationship with drilling mud leakage (Yin and Wu., 2020; Zhao et al., 2020; Li and Li., 2021; Zhao et al., 2021). This study can provide scientific guidance for revealing the wellbore instability mechanism of strike-slip fault zones in similar areas (Jin et al., 1999; Chen et al., 2013; Chen et al., 2015; Gao et al., 2016; Wang et al., 2020; Guo et al., 2021).

GEOLOGICAL SETTING

The Shunbei area is located on the Shuntuoguole Uplift in the central part of the Tarim Basin (**Figure 1**). The structural characteristics of this area are high in the north and low in the south, and high in the east and low in the west. It is a relatively stable ancient tectonic unit in the Tarim Basin. Affected by the

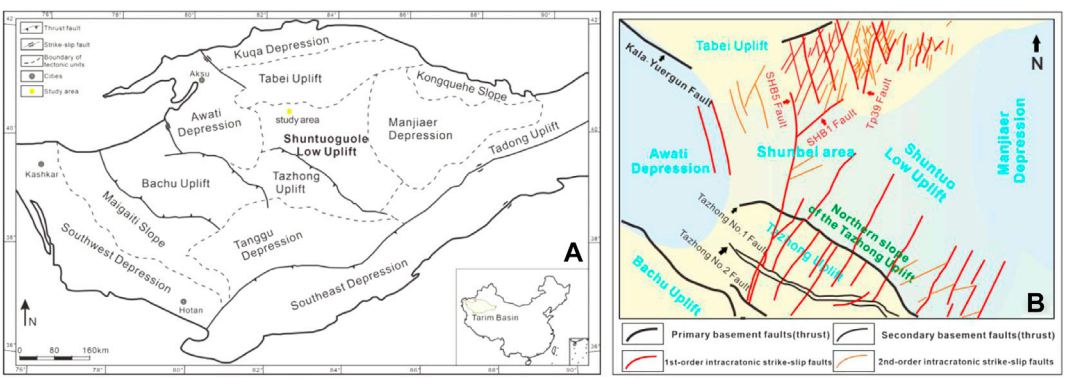

FIGURE 1 | Tectonic location and regional tectonic characteristics of the No. **(A)** Fault Zone in the Shunbei area of Tarim Basin. **(B)** Distribution of faults in the study area.

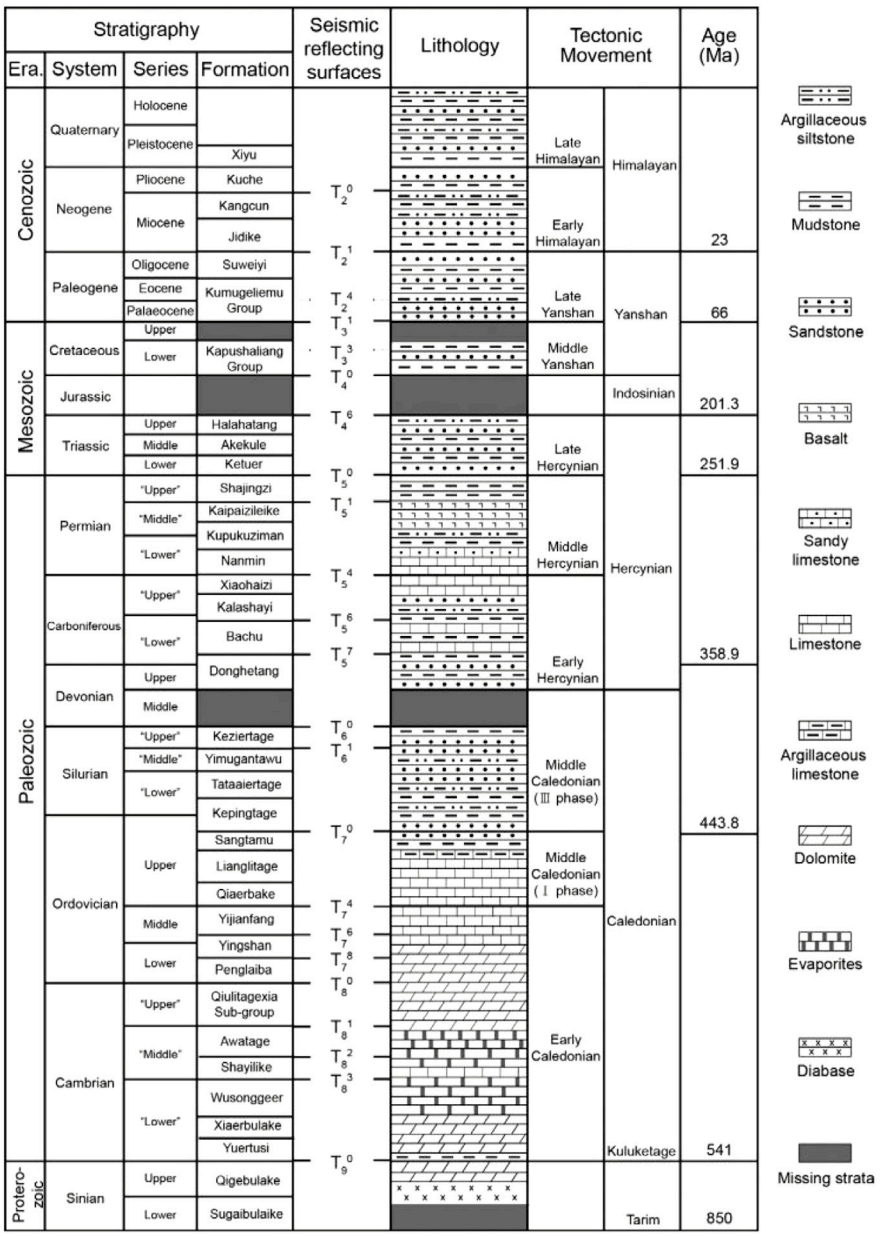

FIGURE 2 | Division of stratigraphic units in the Tarim Basin.

Caledonian, Hercynian, Indosinian, Yanshanian and Himalayan Movements, 18 strike-slip faults in the Shunbei area and its adjacent areas developed in a nearly SN-NE trend. In addition, fault-fracture-type oil and gas reservoirs developed in ultra-deep Ordovician carbonate rocks, and it has been confirmed that these strike-slip fault belts are rich in oil and gas. The Jurassic strata in the Shunbei area are missing; the Cretaceous, Permian, Triassic and Carboniferous strata are partially missing; and other strata are normally developed. From bottom to top, the study area develops Cambrian, Ordovician, Silurian, Devonian, Carboniferous, Permian, Triassic, Cretaceous, Paleogene, Neogene, and Quaternary (**Figure 2**). Among them, the Silurian is the stratum with interbedded sand and mudstone, and the layers with serious leakage of drilling mud are the Lower Silurian Kepingtag Formation and Tata Ertag Formation.

MATERIALS AND METHODS

Materials and Experiments

The data in this study include the Silurian drilling mud leakage data for 19 wells near the strike-slip fault zone in the study area. The specific data include the geological layer at the time of leakage, the section of the leakage well (m), and the lithology; the latter includes

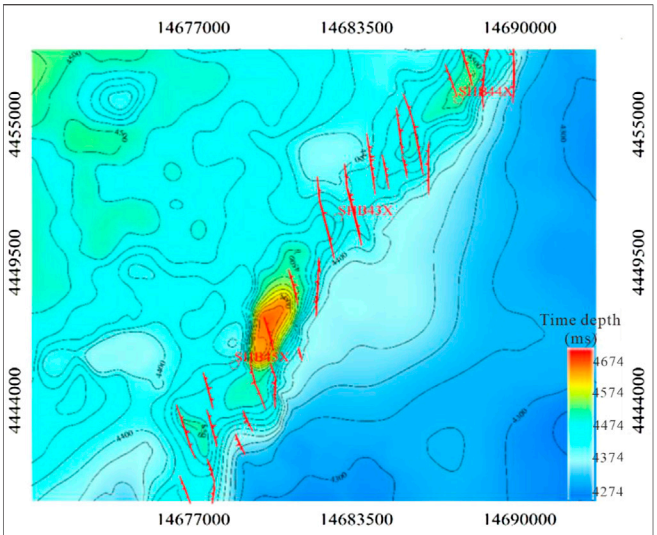

FIGURE 3 | T_6^3 structural contour map of the Silurian in the Shunbei A Strike-Slip Fault Zone in the Tarim Basin.

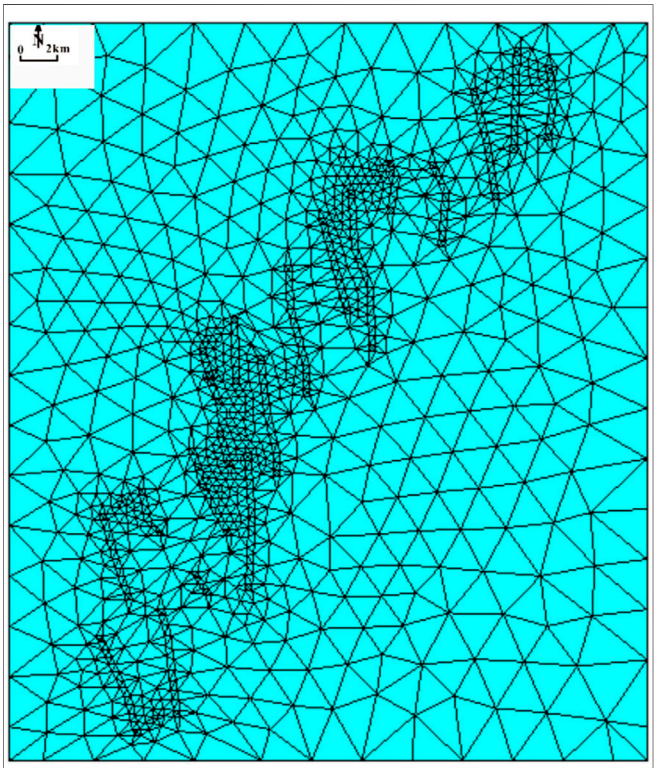

FIGURE 4 | Grid model of Silurian in Shunbei A Strike-Slip Fault Zone in Tarim Basin.

the rate of mud leakage, the cumulative amount of mud leakage (m^3), the density of drilling leakage (g/m^3), and the construction work at the time of mud leakage. In addition, there are three-dimensional (3D) seismic data and interpretation results of the No. A strike-slip fault zone in the Shunbei area. The experimental data includes rock mechanics experiments and acoustic emission (AE) tests.

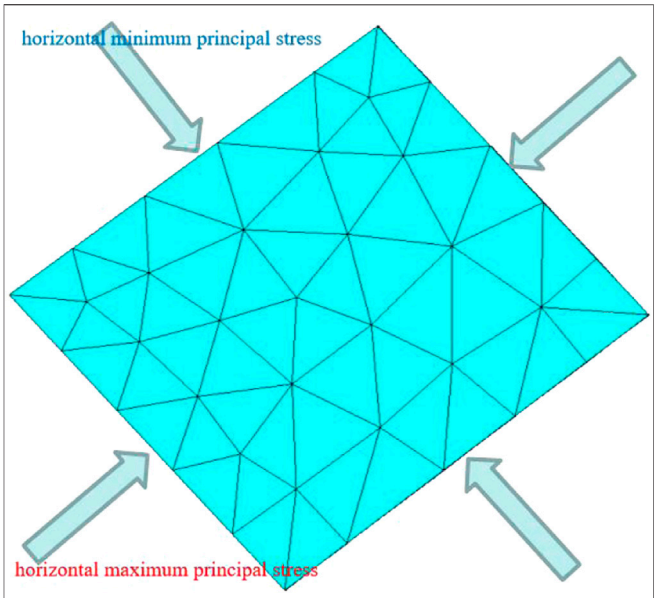

FIGURE 5 | Boundary constraints of numerical simulation of Silurian stress field in Shunbei No. a fault zone.

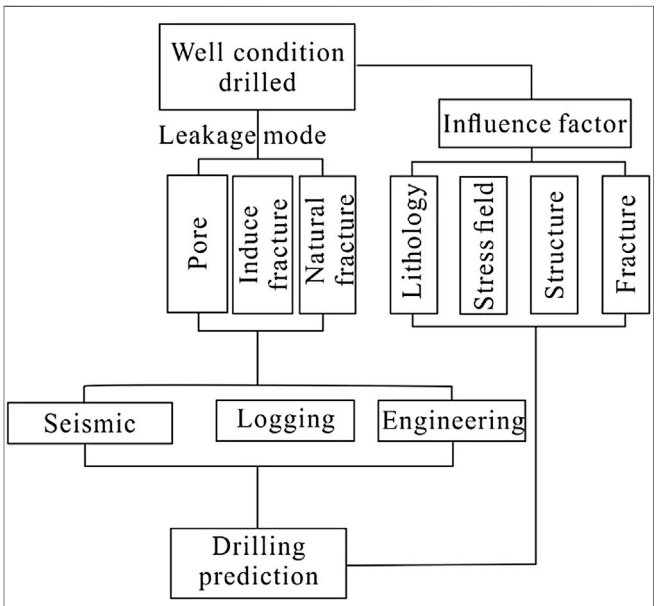

FIGURE 6 | Technical roadmap of strike-slip faults and fractures and their influence on drilling leakage.

Finite Element Method

In this study, the finite element method was used to simulate the tectonic stress field (Ding., et al., 2010; Ding et al., 2012; Jiu et al., 2013; Zeng., et al., 2013; Ding et al., 2016; Liu., et al., 2018). The structural geological model of the northern segment of the Strike-Slip Fault Zone A in the Shunbei area is shown in **Figure 3**, which is subdivided into a series of node and unit grids, including 40,187 nodes and 20,926 grid units (**Figure 4**).

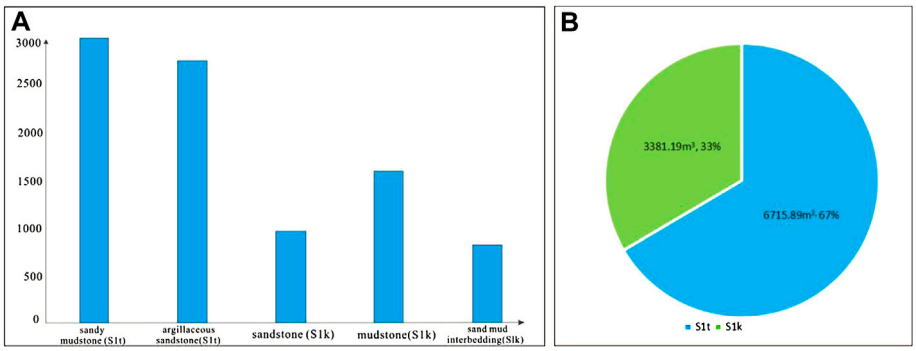

FIGURE 7 | The histogram of the leakage of different layers and lithologies in the Silurian in Shunbei area. **(A)** Leakage of different lithologies; **(B)** Leakage of different strata.

According to the experimental test results of acoustic emission *in-situ* stress, the pressure gradient of the overlying rock of the target layer is 0.0256 MPa/m, the maximum horizontal *in-situ* stress gradient is 0.0234 MPa/m, and the minimum horizontal *in-situ* stress gradient is 0.0187 MPa/m. Finally, we determined that the direction of the maximum horizontal principal stress during the main rupture formation period of the Silurian sand-mudstone stratum was NE-SW, and the direction of the minimum horizontal principal stress was NW-SE (**Figure 5**).

To facilitate the calculation process, the tensile rupture rate I_t and the shear rupture rate I_n are introduced:

$$I_t = \sigma_T/\sigma_t \tag{1}$$

where σ_T is the effective tensile stress, MPa; σ_t is the tensile strength of the rock, MPa. When $I_t \geq 1$, the rock undergoes tension fracture.

$$I_n = \tau_n/|\tau| \tag{2}$$

where τ_n is the effective shear stress, MPa, and $|\tau|$ is the shear strength of the rock, MPa. When $I_n \geq 1$, the rock undergoes shear fracture.

The fracture mode of rock is a comprehensive reflection of tensile stress and shear stress, and a comprehensive fracture coefficient is introduced.

$$I_z = (aI_t + bI_n)/2 \tag{3}$$

In the formula, a and b are the proportions of tension fractures (including tension-shear fractures) and shear fractures obtained from core and electron microscope observations, respectively. In this study a:b = 6:4. Similarly, when $I_z \geq 1$, the rock reaches a fractured state, and the higher the comprehensive fracture rate value, the greater the fracture degree.

R/S-FD Method

R/S analysis, also known as rescaled range analysis or variable scale analysis. This method was originally proposed by British hydrologist Hurst on the basis of long-term research on the relationship between water volume and storage capacity of reservoirs (Hurst, 1951). Through the processing of conventional logging curves by R/S analysis method, the fracture development interval can be preliminarily determined by manually identifying abnormal positions on the R/S curve (Rangarajan and Sant., 2004; Xiao et al., 2019).

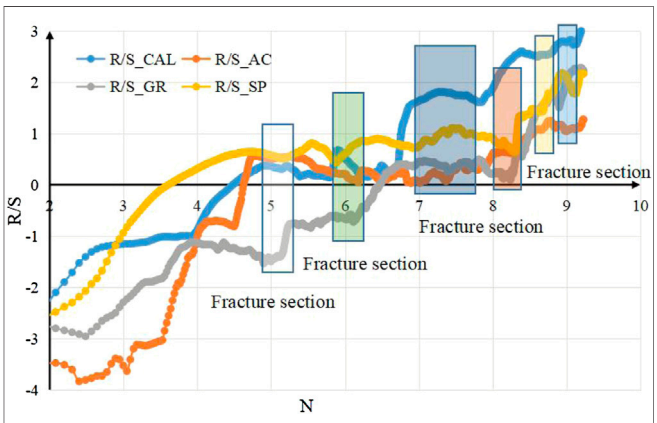

FIGURE 8 | Fracture interval identification based on R/S-FD method in Silurian of Well X in the study area.

In the *R/S* analysis method, *R* is the range, which is the difference between the maximum value and the minimum value, indicating the fluctuation range and complexity of the time series; *S* is called the standard deviation, indicating the average trend of the time series. *R/S* is a dimensionless time series representing fluctuation strength. The calculation methods of *R* and *S* are shown in **formula 4** and **formula 5** respectively:

$$\mathrm{R}(n) = \max_{0<u<n}\left\{\sum_{i=1}^{u} Z(i) - \frac{u}{n}\sum_{i=1}^{u} Z(j)\right\} - \min_{0<u<n}\left\{\sum_{i=1}^{u} Z(i) - \frac{u}{n}\sum_{i=1}^{u} Z(j)\right\} \tag{4}$$

$$\mathrm{S}(n) = \sqrt{\frac{1}{n}\sum_{i=1}^{u} Z^2(i) - \left[\frac{1}{n}\sum_{j=1}^{u} Z(j)\right]^2} \tag{5}$$

$$D = 2 - \frac{\partial LOG\left\{\left[\frac{R(n)}{S(n)}\right], 10\right\}}{\partial n} \tag{6}$$

Among them, Z is a logging curve for *R/S* analysis; n is the number of sampling points in the logging analysis interval (one

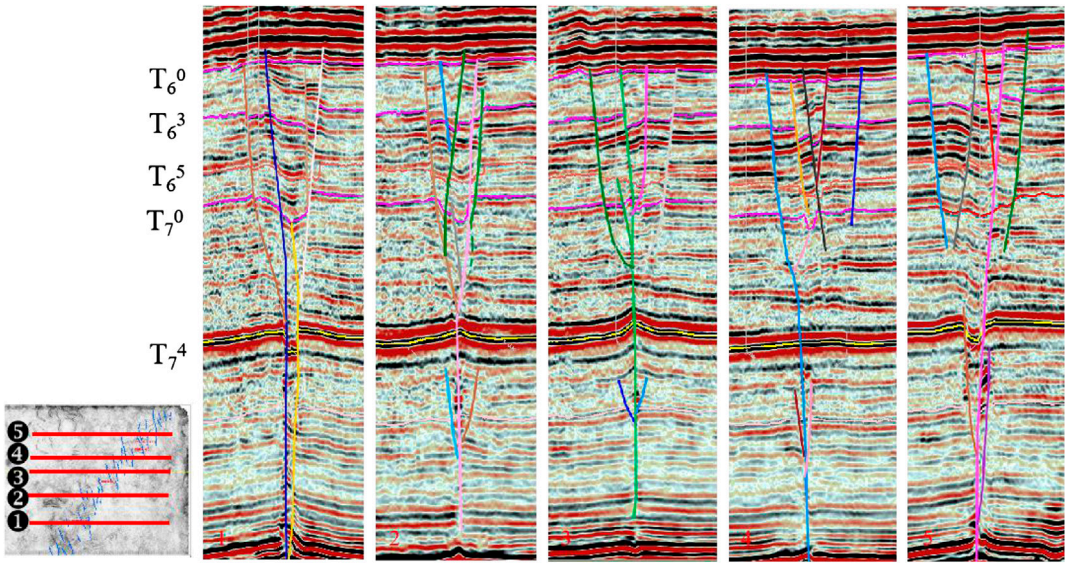

FIGURE 9 | Seismic interpretation profile of the Silurian (T_7^0-T_6^0) negative flower-shaped fault in Shunbei A Fault Zone.

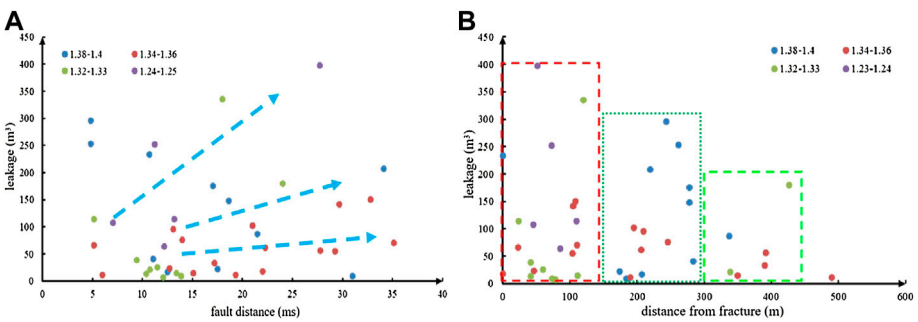

FIGURE 10 | Relationship between Silurian mud leakage and fault throw and its distance from wellbore to fault. **(A)** Relationship between leakage and fault distance; **(B)** Relationship between leakage and distance to fracture.

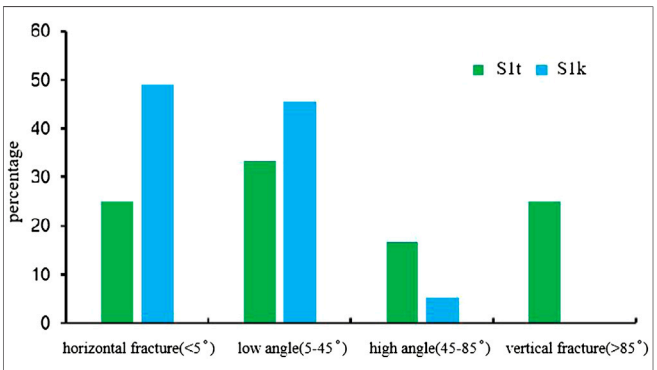

FIGURE 11 | Histogram of dip angle distribution of sandstone core fractures in Well Y in the Silurian of Shunbei area.

sample is taken every 0.125 m), and each n has a corresponding $R(n)/S(n)$ value; u is the number of sampling points increased each time since the beginning; i and j represent variables; D is the fractal dimension, dimensionless, **formula (6)**. Technical roadmap of strike-slip faults and fractures and their influence on drilling leakage is shown in **Figure 6**.

RESULTS

Mud Leakage Characteristics

Statistics on the Silurian mud loss data of 19 wells in the Shunbei area show that in general, the mud loss in S_{1t} is significantly larger than that in S_{1k}. The leakage of sand-bearing mudstone is the largest, followed by mud-bearing sandstone and mudstone layers (**Figure 7**). The mud leakage of each well in different lithologic sections varies greatly.

Log Identification Results of Fractures

R(n)/S(n) is the R/S value corresponding to the nth sampling point. The R/S value and n of each interval are plotted as a logarithmic scatter plot. If the relative change of the two is observed as a densely distributed fitting curve, it indicates that

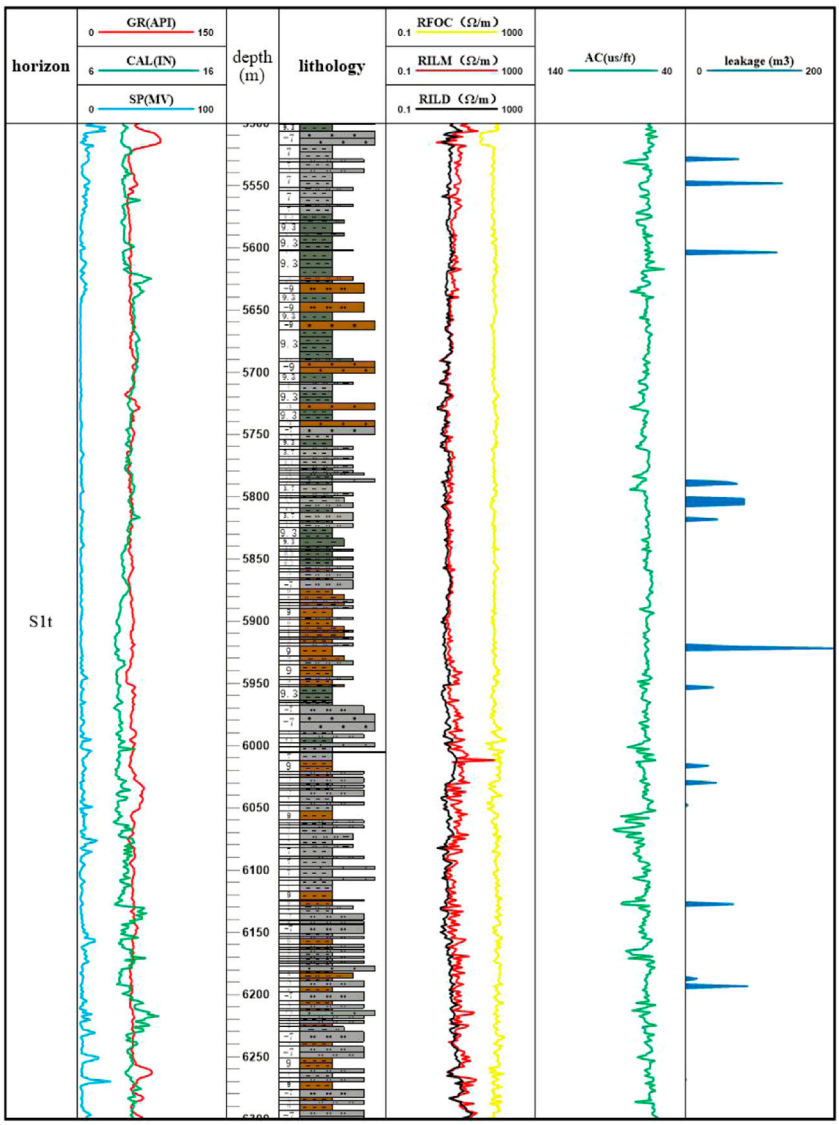

FIGURE 12 | Fracture log identification based on R/S-FD method in target layer of Well Z.

the sequence has good fractal characteristics. The slope H of the R(n)/S(n) curve is called the Hurst exponent. The fractal dimension D of a certain interval can be calculated by **formula (6)**, and its value reflects the heterogeneity of carbonate reservoirs. When some scholars use fractal theory to study the degree of fracture development, they believe that the larger the fractal dimension D, the more developed the fractures (Qie et al., 2021; Wang and Wang., 2021; Wen et al., 2004). The existence of fractures in the formation will lead to a great increase in the complexity of the formation, which corresponds to a higher fractal position value D and a smaller Hurst exponent. The R(n)/S(n) curve shows a decreasing slope segment, which is specifically characterized by the downward shift of the R(n)/S(n) curve. From this, it can be concluded that morphologically, the down-concave segment of the R(n)/S(n) curve can be considered as a potential fracture development segment (**Figure 8**).

Based on the above methods and theories, this paper comprehensively conducts R/S analysis and calculation on five conventional logging curves (CAL, AC, GR, SP and RD) of the Silurian drilling in Shunbei area. If most of the R(n)/S(n) curves show depression in a certain section at the same time, it can indicate that this section is a fracture-developed section. Large errors are usually introduced when manually identifying the concave section of the R(n)/S(n) curve. In order to solve the shortcomings of this method, the second derivative of the function in advanced mathematics is introduced to improve the method. Since the value of R(n)/S(n) is discrete data, this paper uses the finite difference method (FD) to approximate the derivative operation. The logging fracture identification results show that the fracture identification accuracy based on the R/S-FD analysis method can reach 78%.

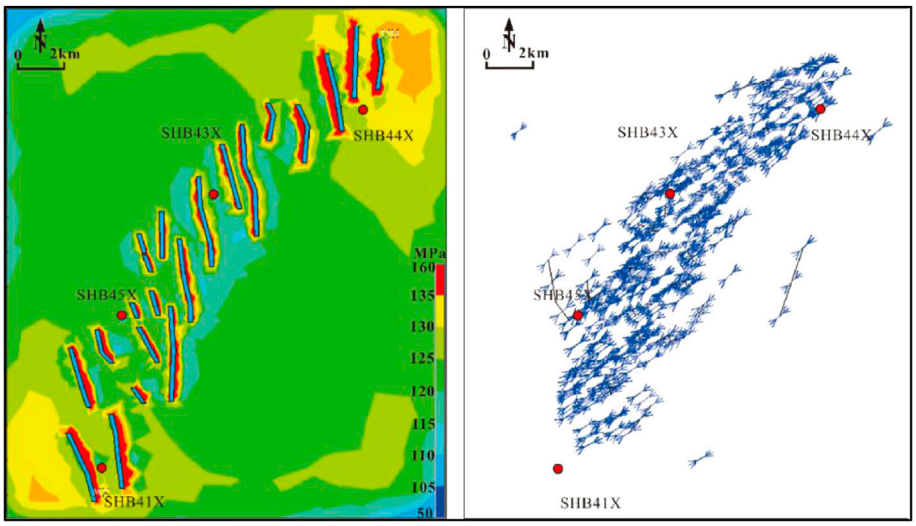

FIGURE 13 | Planar distribution of the maximum principal stress and direction at the T_6^3 interface of the Shunbei No. A Fault Zone.

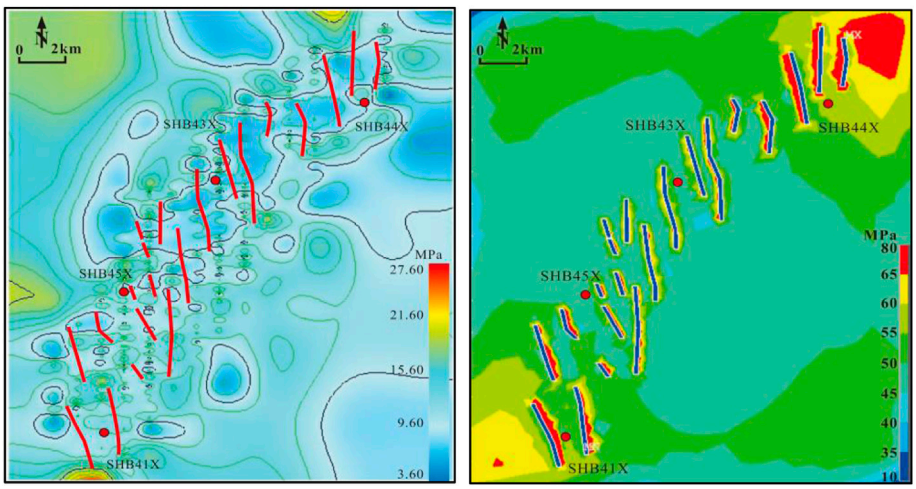

FIGURE 14 | Planar distribution of shear stress and horizontal stress difference at T_6^3 interface of Shunbei No. A Fault Zone.

DISCUSSION

Relationship Between Fault and Mud Leakage

The three-dimensional seismic data can well reflect the fault distribution characteristics of the Silurian system in both vertical and horizontal directions. The faults appear as flower-like structures on the seismic profiles, with obvious strike-slip fault characteristics. The Silurian tectonic layer is an asymmetric negative flower-like tectonic style, with a large number and well-developed strike-slip extensional branch normal faults. The vertical fault throws of main and branch faults are small, reflecting weak extension (**Figure 9**). In addition, the Silurian fault system is mainly arranged in a geese-type normal fault combination pattern on the plane, with a small extension length, and some of them exist in pairs (**Figure 3**).

Nearly north-south extensional negative flower-like branch normal faults are well developed in the study area, which are distributed in a right-order geese pattern, and a few local high points are developed. These features indicate that the Silurian strike-slip extension is strong in the Shunbei area, and the stratum is severely fractured. According to the statistical data of 20 wells, the mud leakage increases with the increase of the fault distance, and the frequency and the leakage volume are the highest when the distance is closer to the fault. Moreover, the leakage frequency is the highest when the wellbore is within 150 m of the fault, followed by 150–300 m. When the wellbore is more than 300 m away from the fault, the likelihood of leakage is lowest (**Figure 10**). The development of negative

TABLE 1 | Criteria for judging the development degree of Silurian fractures in Shunbei area.

Fracture Development Grade	A	B	C
Comprehensive rupture rate IF	IF > 1.4	1.0 < IF < 1.4	IF < 1.0
Fracture development degree	Developed	Relatively developed	Undeveloped

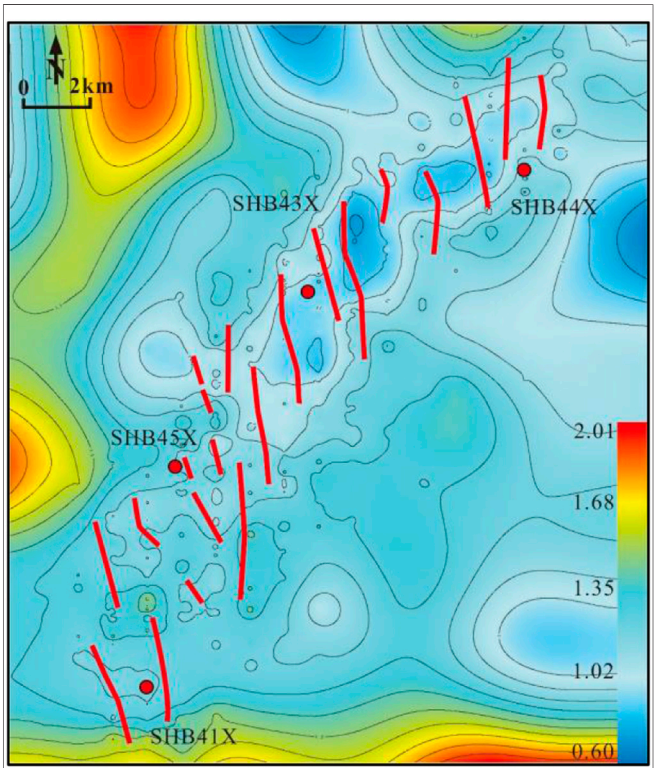

FIGURE 15 | Prediction results of the distribution of Silurian fracture development coefficients in the northern segment of the Shunbei No. A fault zone.

flower-like branch normal faults is the macro-controlling factor of Silurian sand-mudstone formation leakage. The deep tectonic pattern in the study area is shown on the seismic section as a large-angle or near-upright strike-slip fault breaking into the basement, which is mainly developed at the T_7^4 interface (top surface of the middle-lower Ordovician unified Yijianfang Formation) and underlying strata. These faults are formed in one stage.

Relationship Between Fracture Occurrence and Mud Leakage

In Well Shunbei Y, medium and high-angle tension-shear fractures are mainly developed in the sandstone section of the Silurian Tata Ertag Formation (S_{1t}), and low-angle fractures are prone to occur at the sand-mudstone interface. The residues of the invading mud during drilling can be seen on the fracture surfaces of the opened fractures. In addition, Well Shunbei Y mainly developed low-angle fractures in the sandstone section of the Silurian Kalpintag Formation (S_{1k}), and the fractures were mainly generated along weak planes such as horizontal or oblique bedding.

Statistics show that fractures of different dip angles are developed in Silurian S_{1t}, mainly high-angle and vertical fractures. In S_{1k}, low-angle and horizontal fractures are the main factors (**Figure 11**), which is also the main factor causing the mud loss in S_{1t} to be significantly larger than that in S_{1k}.

Relationship Between Vertical Development Characteristics of Fractures and Mud Leakage

Based on the R/S-FD analysis method, this paper uses four logging curves (AC, CAL, SP, GR) to calculate the fractures. Most of the R(n)/S(n) curves show a fracture development segment in the concave curve segment (**Figure 8**, **Figure 12**). And the study found that the fracture development section is in good agreement with the mud leakage section, indicating that the Silurian fracture development is the key factor leading to the leakage.

Tectonic Stress Field and Fracture Distribution and Their Relationship With Mud Leakage

In this study, the finite element method was used to simulate the tectonic stress field and predict the fracture distribution of the Silurian in the Shunbei No. A Fault Zone in the Shunbei area. The maximum principal stress of Shunbei No. A Fault Zone is mainly compressive stress, and its value is concentrated between 115–130 MPa, and it is greatly affected by the fault zone. The stress inside the fault zone is relatively small, and the stress is relatively large near the fault zone (**Figure 13**). The shear stress value of Shunbei No. A Fault Zone is generally positive, ranging from 3.6 to 21.6 MPa. It is reflected that it is dominated by the counterclockwise left-handed shear stress field. In addition, the shear stress values along the main fault zone and its vicinity are larger, and the simulation results are consistent with the deformation characteristics of the compressive-torsional strike-slip structure in the Shunbei area. In addition, the horizontal stress difference range is relatively small (45–60 MPa) within the fault zone, while it is relatively large near the fault zone (**Figure 14**).

In this study, the finite element method was used to calculate the planar distribution of the fracture development coefficient I_F of the Silurian strata in the northern segment of the No. A Fault Zone in the Shunbei area (**Figure 13**). The fracture development coefficient I_F of the Silurian strata in this fault zone is distributed between 0.61 and 2.01. When the I_F of the formation is less than 1, it can be considered that the rock is not fractured. When the I_F of

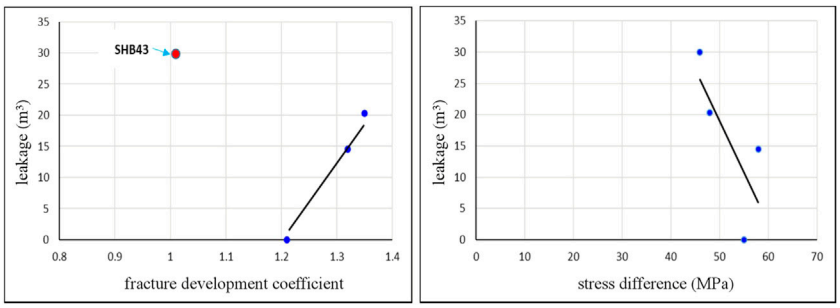

FIGURE 16 | Relationship between Silurian fracture development coefficient, horizontal stress difference and mud leakage in the northern segment of Shunbei No. A fault zone.

the formation is greater than 1, the rocks are fractured to different degrees. The larger the value of I_F, the greater the probability of rock fracture. According to the distribution range of I_F value of Silurian in Shunbei area, it can be divided into three grades A, B and C (**Table 1**). The larger the I_F value and the higher the classification, the easier the rock is to be fractured and the more developed the fractures. In the main fault zone and its vicinity, the fracture development coefficient is between 1.0 and 1.35 (**Figure 15**).

For the four wells drilled on the No. A fault zone in the Shunbei area, we calculated the fracture development coefficient, horizontal stress difference, and their relationship with mud leakage (**Figure 16**). The Silurian as a whole shows that the higher the degree of fracture development, the greater the mud leakage, and the horizontal stress difference is negatively correlated with the mud leakage. For example, Well W3 has a large leakage and a small fracture development coefficient, but the stress difference is small, 46 MPa, which is 2–12 MPa smaller than other stress differences. It shows that the leakage of this well is mainly controlled by *in-situ* stress. The degree of fracture development and the difference in horizontal stress in the Silurian sand-mudstone formation are the main factors leading to high mud leakage.

Through the correlation analysis between the mud leakage and the horizontal stress difference, distance from the fault, and fault distance, it is concluded that the horizontal stress difference is the most direct cause of the mud leakage.

CONCLUSION

(1) In this study, based on 3D seismic, logging, drilling, logging, well log, and engineering construction data, development characteristics of strike-slip faults and fractures, the strength of the *in-situ* stress field, and the influence of these factors on the drilling mud leakage were systematically studied.
(2) The mud leakage in S_{1t} is significantly larger than that in S_{1k}, and the leakage amount in sandy mudstone is the largest; the strong strike-slip extension developed the negative flower-shaped normal faults and the right-order swan-type faults and caused serious stratigraphic fragmentation. The amount of mud leakage increases with the increase of fault distance. Moreover, the closer to the fault, the higher the frequency and amount of mud leakage. When the distance between the wellbore and the fault exceeds 300 m, the possibility of leakage decreases significantly.
(3) The Silurian S_{1t} is dominated by high-angle and vertical tension-shear fractures with good opening; while the S_{1k} is dominated by low-angle structural and horizontal bedding fractures. The difference in fracture type causes the mud leakage in S_{1t} to be significantly larger than that of S_{1k}.
(4) The fracture development intervals identified by the R/S-FD method are in good agreement with the mud leakage intervals, which further indicates that the degree of fracture development is the key factor leading to the drilling mud leakage.
(5) The degree of fracture development and the difference in horizontal principal stresses are the dominant factors leading to high Silurian mud leakage. Mud leakage has significant positive and negative correlations with the fracture development coefficient and the horizontal stress difference, respectively.

DATA AVAILABILITY STATEMENT

The original contributions presented in the study are included in the article/supplementary material further inquiries can be directed to the corresponding author.

AUTHOR CONTRIBUTIONS

HL is responsible for the idea, seismic/logging data interpretation and writing of this paper.

FUNDING

This research was supported by the National Natural Science Foundation of China (Grant No. 42072173) and the scientific research project (KY2020-S-030) of Sinopec Northwest Oilfield Company.

REFERENCES

Al-Ajmi, A. M., and Zimmerman, R. W. (2006). Stability Analysis of Vertical Boreholes Using the Mogi-Coulomb Failure Criterion. *Int. J. Rock Mech. Min. Sci.* 43 (8), 1200–1211. doi:10.1016/j.ijrmms.2006.04.001

Chen, Z., Zhang, H., Shen, B., Yin, G., and Wang, X. (2013). A Study on Safe and Dangerous Drilling Azimuths of Horizontal Well. *Acta Pet. Sin.* 34 (1), 164–168. doi:10.7623/syxb201301021

Chen, P., Ma, T., and Xia, H. (2014). A Collapse Pressure Prediction Model of Horizontal Shalegas Wells with Multiple Weak Planes. *Nat. Gas. Ind.* 34 (12), 87–93. doi:10.3787/j.issn.1000-0976.2014.12.012

Chen, P., Ma, T., and Fan, X. (2015). Well Path Optimization Based on Wellbore Stability Analysis. *Nat. Gas. Ind.* 35 (10), 84–92. doi:10.3787/j.issn.1000-0976.2015.10.011

Chen, G. B., Li, T., Yang, L., Zhang, G. H., Li, J. W., and Dong, H. J. (2021). Mechanical Properties and Failure Mechanism of Combined Bodies with Different Coal-Rock Ratios and Combinations. *J. Min. Strata Control Eng.* 3 (2), 023522. doi:10.13532/j.jmsce.cn10-1638/td.20210108.001

Ding, W., Fan, T., Huang, X., and Liu, C. (2010). Paleo-structural Stress Field Simulation for Middle-Lower Ordovician in Tazhong Area and Favorable Area Prediction of Fractured Reservoirs. *J. China Univ. Petroleum* 34 (5), 1–6. doi:10.3969/j.issn.1673-5005.2010.05.001

Ding, W., Fan, T., Yu, B., Huang, X., and Liu, C. (2012). Ordovician Carbonate Reservoir Fracture Characteristics and Fracture Distribution Forecasting in the Tazhong Area of Tarim Basin, Northwest China. *J. Petroleum Sci. Eng.* 86-87, 62–70. doi:10.1016/j.petrol.2012.03.006

Ding, W., Zeng, W., Wang, R., Jiu, K., Wang, Z., Sun, Y., et al. (2016). Method and Application of Tectonic Stress Field Simulation and Fracture Distribution in Shale Reservoir. *Earth Sci. Front.* 23 (2), 63–74. doi:10.13745/j.esf.2016.02.008

Deng, S., Li, H., Zhang, Z., Wu, X., and Zhang, J. (2018). Characteristics of Differential Activities in Major Strike-Slip Fault Zones and Their Control on Hydrocarbon Enrichment in Shunbei Area and its Surroundings, Tarim Basin. *Oil Gas Geol.* 39 (05), 878–888. doi:10.11743/ogg20180503

Deng, S., Li, H., Zhang, Z., Zhang, J., and Yang, X. (2019a). Structural Characterization of Intracratonic Strike-Slip Faults in the Central Tarim Basin. *Bulletin* 103 (1), 109–137. doi:10.1306/06071817354

Deng, S., Li, H., Han, J., Cui, D., and Zou, R. (2019b). Characteristics of the Central Segment of Shunbei 5 Strike-Slip Fault Zone in Tarim Basin and its Geological Significance. *Oil Gas Geol.* 40 (05), 990–998+1073. doi:10.11743/ogg20190504

Ding, F., Xie, C., Zhou, X., Jiang, C., Li, K., Wan, L., et al. (2021). Defining Stratigraphic Oil and Gas Plays by Modifying Structural Plays: A Case Study from the Xihu Sag, East China Sea Shelf Basin. *Energy Geosci.* 2 (1), 41–51. doi:10.1016/j.engeos.2020.08.002

Fan, C., Li, H., Qin, Q., He, S., and Zhong, C. (2020). Geological Conditions and Exploration Potential of Shale Gas Reservoir in Wufeng and Longmaxi Formation of Southeastern Sichuan Basin, China. *J. Petroleum Sci. Eng.* 191, 107138. doi:10.1016/j.petrol.2020.107138

Gao, F. Q. (2021). Influence of Hydraulic Fracturing of Strong Roof on Mining-Induced Stress Insight from Numerical Simulation. *J. Min. Strata Control Eng.* 3 (2), 023032. doi:10.13532/j.jmsce.cn10-1638/td.20210329.001

Gao, J., Deng, J., Yan, W., Feng, Y., Wang, H., and Li, Y. (2016). Establishment of Apredictionn Model for the Borehole Trajactory Optimization Based on Controlling Wellbore Stability. *Acta Pet. Sin.* 37, 1179–1186. doi:10.7623/syxb201609013

Guo, L. L., Zhou, D. W., Zhang, D. M., and Zhou, B. H. (2021). Deformation and Failure of Surrounding Rock of a Roadway Subjected to Mining-Induced Stresses. *J. Min. Strata Control Eng.* 3 (2), 023038. doi:10.13532/j.jmsce.cn10-1638/td.20200727.001

Han, J., Kuang, A., Neng, Y., Huang, C., Li, Q., Chen, P., et al. (2016). Vertical Layered Structure of Shunbei No.5 Strike-Slip Fault Zone and its Significance on Hydrocarbon Accumulation. *Xingjiang Pet. Geol.* 42 (02), 152–160. doi:10.7657/XJPG20210204

He, X., Zhang, P., He, G., Gao, Y., Liu, M., Zhang, Y., et al. (2020). Evaluation of Sweet Spots and Horizontal-Well-Design Technology for Shale Gas in the Basin-Margin Transition Zone of Southeastern Chongqing, SW China. *Energy Geosci.* 1 (3–4), 134–146. doi:10.1016/j.engeos.2020.06.004

Hower, J. C., and Groppo, J. G. (2021). Rare Earth-Bearing Particles in Fly Ash Carbons: Examples from the Combustion of Eastern Kentucky Coals. *Energy Geosci.* 2 (2), 90–98. doi:10.1016/j.engeos.2020.09.003

Hurst, H. E. (1951). Long-term Storage Capacity of Reservoirs. *Trans. Am. Soc. Civ. Eng.* 116 (1), 770–799. doi:10.1061/TACEAT.0006518

Jiao, F. (2017). Significance of Oil and Gas Exploration in NE Strike-Slip Fault Belts in Shuntuoguole Area of Tarim Basin. *Oil Gas Geol.* 38 (05), 831–839. doi:10.11743/ogg20170501

Jiao, F. (2018). Significance and Prospect of Ultra-deep Carbonate Fault-Karst Reservoirs in Shunbei Area, Tarim Basin. *Oil Gas Geol.* 39 (02), 207–216. doi:10.11743/ogg20180201

Jin, Y., Chen, M., Liu, G., and Chen, Z. (1999). Wellbors Stability Analysis of Extended Reach Wells. *J. Geomechanics* 5 (1), 1–4. doi:10.3969/j.issn.1006-6616.1999.01.002

Jiu, K., Ding, W., Huang, W., You, S., Zhang, Y., and Zeng, W. (2013). Simulation of Paleotectonic Stress Fields within Paleogene Shale Reservoirs and Prediction of Favorable Zones for Fracture Development within the Zhanhua Depression, Bohai Bay Basin, East China. *J. Petroleum Sci. Eng.* 110, 119–131. doi:10.1016/j.petrol.2013.09.002

Li, D., Kang, Y., Liu, S., Zeng, Y., and Du, C. (2011). Leakage Pressure Model of Carbonate Formation Based on Leakage Mechanism. *ACTA PET. SIN.* 32 (5), 5. doi:10.7623/syxb201105026

Li, H., Tang, H., Qin, Q., Zhou, J., Qin, Z., Fan, C., et al. (2019). Characteristics, Formation Periods and Genetic Mechanisms of Tectonic Fractures in the Tight Gas Sandstones Reservoir: A Case Study of Xujiahe Formation in YB Area, Sichuan Basin, China. *J. Petroleum Sci. Eng.* 178, 723–735. doi:10.1016/j.petrol.2019.04.007

Li, H., Qin, Q., Zhang, B., Ge, X., Hu, X., Fan, C., et al. (2020). Tectonic Fracture Formation and Distribution in Ultradeep Marine Carbonate Gas Reservoirs: A Case Study of the Maokou Formation in the Jiulongshan Gas Field, Sichuan Basin, Southwest China. *Energy fuels..* 34 (11), 14132–14146. doi:10.1021/acs.energyfuels.0c03327

Li, H. (2022). Research Progress on Evaluation Methods and Factors Influencing Shale Brittleness: A Review. *Energy Rep.* 8, 4344–4358. doi:10.1016/j.egyr.2022.03.120

Li, L., and Li, S. J. (2021). Evolution Rule of Overlying Strata Structure in Repeat Mining of Shallow Close Distance Seams Based on Schwarz Alternating Procedure. *J. Min. Strata Control Eng.* 3 (2), 023515. doi:10.13532/j.jmsce.cn10-1638/td.20210225.001

Liu, J., Ding, W., Dai, J., Wu, Z., and Yang, H. (2018). Quantitative Prediction of Lower Order Faults Based on the Finite Element Method: A Case Study of the M35 Fault Block in the Western Hanliu Fault Zone in the Gaoyou Sag, East China. *Tectonics* 37 (10), 3479–3499. doi:10.1029/2017TC004767

Mohammed, B., Richard, H. W., Shettima, B., and Philip, S. (2021). Diagenesis and its Controls on Reservoir Quality of the Tambar Oil Field, Norwegian North Sea. *Energy Geosci.* 2 (1), 10–31. doi:10.1016/j.engeos.2020.07.002

Qi, L., Yun, L., Cao, Z., Li, H., and Huang, C. (2021). Geological Reserves Assessment and Petroleum Exploration Targets in Shunbei Oil & Gas Field. *Xingjiang Pet. Geol.* 42 (02), 127–135. doi:10.7657/XJPG20210201

Qie, L., Shi, Y. N., and Liu, J. S. (2021). Experimental Study on Grouting Diffusion of Gangue Solid Filling Bulk Materials. *J. Min. Strata Control Eng.* 3 (2), 023011. doi:10.13532/j.jmsce.cn10-1638/td.20201111.001

Rangarajan, G., and Sant., D. A. (2004). Fractal Dimensional Analysis of Indian Climatic Dynamics. *Chaos, Solit. Fractals* 19 (2), 285–291. doi:10.1016/S0960-0779(03)00042-0

Santosh, M., and Feng, Z. Q. (2020). New Horizons in Energy Geoscience. *Energy Geosci.* 1 (1–2), 1–2. doi:10.1016/j.engeos.2020.05.005

Wang, H., Shi, Z., Zhao, Q., Liu, D., Sun, S., Guo, W., et al. (2020). Stratigraphic Framework of the Wufeng-Longmaxi Shale in and Around the Sichuan Basin, China: Implications for Targeting Shale Gas. *Energy Geosci.* 1 (3–4), 124–133. doi:10.1016/j.engeos.2020.05.006

Wang, J., and Wang, X. L. (2021). Seepage Characteristic and Fracture Development of Protected Seam Caused by Mining Protecting Strata. *J. Min. Strata Control Eng.* 3 (3), 033511. doi:10.13532/j.jmsce.cn10-1638/td.20201215.001

Wen, H., Xiao, C., Li, R., Yang, B., and Wang, H. (2004). On Multifractal Analysis Method in Well Logging Interpretation. *Well Logging Technol.* 28 (5), 381–385. doi:10.16489/j.issn.1004-1338.2004.05.004

Xiao, Z., Ding, W., Liu, J., Tian, M., Yin, S., Zhou, X., et al. (2019). A Fracture Identification Method for Low-Permeability Sandstone Based on R/S Analysis and the Finite Difference Method: A Case Study from the Chang 6 Reservoir in

Huaqing Oilfield, Ordos Basin. *J. Petroleum Sci. Eng.* 174, 1169–1178. doi:10.1016/j.petrol.2018.12.017

Xue, F., Liu, X. X., and Wang, T. Z. (2021). Research on Anchoring Effect of Jointed Rock Mass Based on 3D Printing and Digital Speckle Technology. *J. Min. Strata Control Eng.* 3 (2), 023013. doi:10.13532/j.jmsce.cn10-1638/td.20201020.001

Yan, C., and Zhao, K. (2018). *New Technology for Evaluating Wellbore Stability in Complex Strata*. Beijing: Sinopec Press, 1–2.

Yin, S., Ding, W., Yang, W., Zhao, W., Zhang, M., and Cong, S. (2015). Progress of Borehole Stability Considering Strata Anisotropy. *Adv. Earth Sci.* 30, 13–25. doi:10.11867/j.issn.1001-8166.2015.11.1218

Yin, S., Lv, D. W., and Ding, W. L. (2018). New Method for Assessing Microfracture Stress Sensitivity in Tight Sandstone Reservoirs Based on Acoustic Experiments. *Int. J. Geomechanics* 18 (4), 1–16. doi:10.1061/(asce)gm.1943-5622.0001100

Yin, S., Dong, L., Yang, X., and Wang, R. (2020). Experimental Investigation of the Petrophysical Properties, Minerals, Elements and Pore Structures in Tight Sandstones. *J. Nat. Gas Sci. Eng.* 73, 1–14. doi:10.1016/j.jngse.2020.103189

Yin, S., and Wu, Z. (2020). Geomechanical Simulation of Low-Order Fracture of Tight Sandstone. *Mar. Petroleum Geol.* 100, 1–16. doi:10.1016/j.marpetgeo.2020.104359

Zeng, W., Ding, W., Zhang, J., Zhang, Y., Guo, L., Jiu, K., et al. (2013). Fracture Development in Paleozoic Shale of Chongqing Area (South China). Part Two: Numerical Simulation of Tectonic Stress Field and Prediction of Fractures Distribution. *J. Asian Earth Sci.* 75, 267–279. doi:10.1016/j.jseaes.2013.07.015

Zhan Zhao, Z., Liu, J., Ding, W., Yang, R., and Zhao, G. (2021). Analysis of Seismic Damage Zones: A Case Study of the Ordovician Formation in the Shunbei 5 Fault Zone, Tarim Basin, China. *J. Mar. Sci. Eng.* 9 (6), 630. doi:10.3390/JMSE9060630

Zhao, R., Zhao, T., Li, H., Deng, S., and Zhang, J. (2019). Fault-Controlled Fracture-Cavity Reservoir Characterization and Main-Controlling Factors in the Shunbei Hydrocarbon Field of Tarim Basin. *Special Oil Gas Reservoirs* 26 (05), 8–13. doi:10.3969/j.issn.1006-6535.2019.05.002

Zhao, Z., Wu, K., Fan, Y., Guo, J., Zeng, B., and Yue, W. (2020). An Optimization Model for Conductivity of Hydraulic Fracture Networks in the Longmaxi Shale, Sichuan Basin, Southwest China. *Energy Geosci.* 1 (1–2), 47–54. doi:10.1016/j.engeos.2020.05.001

Zhao, K. K., Jiang, P. F., Feng, Y. J., Sun, X. D., Cheng, L. X., and Zheng, J. W. (2021). Investigation of the Characteristics of Hydraulic Fracture Initiation by Using Maximum Tangential Stress Criterion. *J. Min. Strata Control Eng.* 3 (2), 023520. doi:10.13532/j.jmsce.cn10-1638/td.20201217.001

Zheng, H., Zhang, J., and Qi, Y. (2020). Geology and Geomechanics of Hydraulic Fracturing in the Marcellus Shale Gas Play and Their Potential Applications to the Fuling Shale Gas Development. *Energy Geosci.* 1 (1–2), 36–46. doi:10.1016/j.engeos.2020.05.002

Conflict of Interest: Author HL was employed by the Sinopec Northwest Oilfield Branch.

The remaining author declares that the research was conducted in the absence of any commercial or financial relationships that could be construed as a potential conflict of interest.

Publisher's Note: All claims expressed in this article are solely those of the authors and do not necessarily represent those of their affiliated organizations, or those of the publisher, the editors and the reviewers. Any product that may be evaluated in this article, or claim that may be made by its manufacturer, is not guaranteed or endorsed by the publisher.